

**GC-globulin/vitamin D-binding protein is required for pancreatic  $\alpha$  cell adaptation to metabolic stress**

Katrina Vilorio<sup>1,2</sup>, Daniela Nasteska<sup>1,2</sup>, Julia Ast<sup>1,2</sup>, Annie Hasib<sup>1,2</sup>, Federica Cuzzo<sup>1,2</sup>, Silke Heising<sup>1,2</sup>, Linford J.B. Briant<sup>3</sup>, Martin Hewison<sup>1,2\*</sup>, David J. Hodson<sup>1,2,3\*</sup>

<sup>1</sup> Institute of Metabolism and Systems Research (IMSR), and Centre of Membrane Proteins and Receptors (COMPARE), University of Birmingham, Birmingham, UK.

<sup>2</sup> Centre for Endocrinology, Diabetes and Metabolism, Birmingham Health Partners, Birmingham, UK.

<sup>3</sup> Oxford Centre for Diabetes, Endocrinology and Metabolism (OCDEM), NIHR Oxford Biomedical Research Centre, Churchill Hospital, Radcliffe Department of Medicine, University of Oxford, Oxford, OX3 7LE, UK.

\*Correspondence should be addressed to:

[m.hewison@bham.ac.uk](mailto:m.hewison@bham.ac.uk), [david.hodson@ocdem.ox.ac.uk](mailto:david.hodson@ocdem.ox.ac.uk)

**Word count:**

**Keywords:** GC-globulin, vitamin D-binding protein,  $\alpha$  cell, alpha cell, glucagon, type 2 diabetes, obesity

## ABSTRACT

GC-globulin (GC), or vitamin D-binding protein, is a multifunctional protein involved in transport of circulating vitamin 25(OH)D and fatty acids, as well as actin-scavenging. In the pancreatic islets, the gene encoding GC, *GC*, is highly-localized to glucagon-secreting  $\alpha$  cells. Despite this, the role of GC in  $\alpha$  cell function is poorly understood. We previously showed that GC is essential for  $\alpha$  cell morphology, electrical activity and glucagon secretion. We now show that loss of GC exacerbates  $\alpha$  cell failure during metabolic stress. High fat diet-fed *GC*<sup>-/-</sup> mice have basal hyperglucagonemia, which is associated with decreased  $\alpha$  cell size, impaired glucagon secretion and  $\text{Ca}^{2+}$  fluxes, and changes in glucose-dependent F-actin remodelling. Impairments in glucagon secretion can be rescued using exogenous GC to replenish  $\alpha$  cell GC levels, increase glucagon granule area and restore the F-actin cytoskeleton. Lastly, GC levels decrease in  $\alpha$  cells of donors with type 2 diabetes, which is associated with changes in  $\alpha$  cell mass, morphology and glucagon expression. Together, these data demonstrate an important role for GC in  $\alpha$  cell adaptation to metabolic stress.

**Brief Summary:** GC-globulin/vitamin D-binding protein protects pancreatic  $\alpha$  cells from metabolic stress, maintaining glucagon secretion.

## INTRODUCTION

During metabolic stress,  $\alpha$  cell function becomes dysregulated, leading to inappropriate glucagon secretion and exacerbation of blood glucose levels (1), as well as impaired counter-regulatory responses (2). The mechanisms involved are multifactorial and include changes in  $\alpha$  cell glucose-sensing,  $\alpha$  cell de-differentiation, paracrine feedback, hyperaminoacidemia, as well as  $\alpha$  cell mass (3-8). The importance of glucagon during metabolic stress and diabetes is exemplified by studies showing that deletion or blockade of the glucagon receptor protects against diabetes (9; 10), and that immunoneutralization of glucagon restores glucose homeostasis in STZ-treated rats (11) or obese mice (12).

GC globulin (GC), also known as vitamin D-binding protein, is an ~58 kDa glycosylated  $\alpha$  protein that transports vitamin D metabolites and fatty acids in the circulation (13; 14). GC is also amongst the most potent actin scavengers in the body and acts in concert with gelsolin to sequester actin filaments released from lysed cells (15; 16). *GC/Gc*, the gene encoding GC, was thought to be almost exclusively expressed in the liver, where sterol-derivatives such as cholecalciferol are converted into pre-hormone 25-OH vitamin D (25(OH)D) (17). However, recent studies have shown that human and mouse  $\alpha$  cells express equally high levels of *GC/Gc* (18; 19), whereas the gene is absent from  $\beta$  cells (19; 20). Notably, GC constitutes an  $\alpha$  cell signature gene, since its promoter region is enriched for cell type-selective open chromatin regions (18). Moreover, a large-scale Mendelian randomization study of European and Chinese adults has revealed associations between GC single nucleotide polymorphisms (SNPs) and T2D risk (21). Despite this, the tissue-specific mechanisms by which GC influences metabolic traits are poorly characterized.

Recently, we showed that GC contributes to the maintenance of  $\alpha$  cell function (22; 23). Deletion of GC leads to smaller and hyperplastic  $\alpha$  cells, which display abnormal  $\text{Na}^+$  conductance,  $\text{Ca}^{2+}$  fluxes and glucagon secretion. This effect was found to be mediated by changes in the F-actin cytoskeleton, with a large increase in microfilament thickness and

density in GC<sup>-/-</sup> islets. Notably, up until this point, actin-binding properties of GC had only been described in the circulation. These studies were recently corroborated by Patch-seq studies where GC was shown to inversely correlate with peak Na<sup>+</sup> current in human  $\alpha$  cells (8). Despite the role of GC in maintaining  $\alpha$  cell identity, it remains unknown how GC impacts  $\alpha$  cell responses to metabolic stress. Studies have suggested that manipulation of GC levels is able to restore glucose homeostasis in obese mouse models, although the exact cellular mechanisms are unclear, as GC is upregulated in de-differentiated  $\beta$  cells (24). Although GC is an  $\alpha$  cell signature gene, it is also unclear if abundant circulating levels of GC may also impact glucagon secretion and  $\alpha$  cell function.

In the present study, we set out to understand the role of GC in  $\alpha$  cell function during metabolic stress. By combining GC<sup>-/-</sup> mice and pancreas sections from type 2 diabetes (T2D) donors with immunohistochemistry, live imaging and high-resolution microscopy, we show that GC is required for  $\alpha$  cell function and glucagon secretion under diabetogenic conditions. Pertinently,  $\alpha$  cell dysfunction can be rescued by restoring GC levels using exogenous protein.

## **RESEARCH DESIGN AND METHODS**

### **Experimental design**

No data were excluded unless the cells failed to respond to positive control, responded inappropriately to negative control, or displayed impaired viability. All individual data points are reported. The measurement unit is animal or batch of islets or pancreas section, with experiments replicated independently. Animals and islets were randomly allocated to treatment groups to ensure that all states were represented in the different experiment arms. Animals and pancreas sections were coded to allow blinded analysis.

### **Mouse models**

GC<sup>-/-</sup> mice harboring deletion of exon 5 of the GC gene were backcrossed to C57BL/6J for 10 generations (25). These mice have undetectable circulating GC, as well as 25(OH)[3H]D3 binding (22; 25). Mice were housed in a specific pathogen-free facility with ad lib access to food and water. Vitamin D sufficiency was ensured by using chow supplemented with 1000 U/kg cholecalciferol. Mice were fed standard chow (SC) or high fat diet (HFD) containing 60% fat (Research Diets, Catalog# D12492), and body weight checked weekly from 0 to 12 weeks. Male and female mice were placed on SC or HFD from 8 weeks of age (numbers reported in the figure legends).

### **Human donors**

Formalin-fixed paraffin-embedded pancreas sections were obtained from the Alberta Diabetes Institute IsletCore. Quality control and phenotyping data is available for each preparation via [www.isletcore.ca](http://www.isletcore.ca).

### **Glucose and insulin tolerance tests**

Mice were fasted for 4-5 hours (8:00 am- 12:30 pm) before intraperitoneal injection of 1.5g/kg of sterile filtered D-glucose. Tail vein sampling was performed at 0, 15, 30, 60, 90 and 120

mins post injection. Glucose levels were measured using a Contour XT glucometer (Bayer). For plasma glucagon measures, mice were fasted for 4-5 hours (8:00 am- 12:30 pm) before intraperitoneal injection of 0.75U/kg of insulin (Lilly, Humulin S). Blood was collected at 0 and 30 mins post injection and stored at -80°C pending ELISA for serum glucagon (Mercodia, Catalog# 10-1281-01). Values lower than the assay detection limit were interpolated from the standard.

#### **Islet isolation and culture**

Mice were humanely euthanized by rising CO<sub>2</sub> and cervical dislocation (Schedule 1), before bile duct injection and inflation of the pancreas with 1 mg/ml SERVA NB8 collagenase (Amsbio, Catalog# 17456.02). Islets were purified using Ficoll-Paque (Cytiva, Catalog# 17144003) or Histopaque (Sigma-Aldrich, Catalog# 11191, Catalog# 10831) gradient separation and maintained at 37°C and 5% CO<sub>2</sub> in RPMI 1640 medium (Gibco, Catalog# 21875034) containing 10% FCS (Sigma-Aldrich, Catalog# F9665), 100 units/mL penicillin, and 100 µg/mL streptomycin (Gibco Catalog# 15140122).

#### **Immunostaining of mouse pancreases**

Pancreases harvested before overnight incubation with 10% formalin overnight and dehydration and wax embedding. Sections were cut at 5 µm using a Leica microtome, before de-paraffinization and blocking with PBS-T + 1% BSA for 1 hour. Sections were incubated with primary antibodies overnight at 4°C, before washing in PBS-T + 0.1% BSA (Sigma-Aldrich, Catalog# A3803) and incubation with secondary antibodies for 2 hours at room temperature.

Primary antibodies used were: rabbit anti-insulin 1:500 (Cell Signaling Technology, Catalog# 3014, RRID:AB\_2126503); mouse monoclonal anti-glucagon 1:2000 (Sigma-Aldrich, Catalog# G2654, RRID:AB\_259852); mouse anti-somatostatin 1:1000 (Thermo Fisher Scientific, Catalog#14-9751-80, RRID:AB\_2572981) and rabbit anti-DBP 1:1000 (Sigma-Aldrich, Catalog# HPA019855, RRID:AB\_1849545). Secondary antibodies were: goat anti-

rabbit Alexa Fluor 633 (Thermo Fisher Scientific, Catalog# A-21052, RRID:AB\_2535719), goat anti-rabbit Alexa Fluor 488 (Thermo Fisher Scientific, Catalog# R37116, RRID:AB\_2556544), goat anti-guinea pig Alexa Fluor 488 (Thermo Fisher Scientific, Catalog# A-11073, RRID:AB\_2534117), goat anti-mouse Alexa Fluor 488 (Thermo Fisher Scientific, Catalog# A-11029, RRID:AB\_138404) and goat anti-guinea pig Alexa Fluor 568 (Thermo Fisher Scientific, Catalog# A-11075, RRID:AB\_2534119), applied at 1:1000. Specificity of antibodies was based upon known cell type co-localizations, overlap with insulin, glucagon or somatostatin reporters, or loss of staining in knockout tissue. F-actin and G-actin were visualized using Phalloidin-488 (Abcam, Catalog# ab176753) or DNase1-594 (Invitrogen, Catalog# D12372), respectively.

Imaging was performed using either Zeiss LSM780 or LSM880 meta-confocal microscopes, equipped with sensitive GaAsP spectral detectors. Alexa Fluor 488, Alexa Fluor 568 and Alexa Fluor 633 were excited at  $\lambda = 488$  nm,  $\lambda = 568$  and  $\lambda = 633$  nm, respectively. Emitted signals for Alexa Fluor 488, Alexa Fluor 568 and Alexa Fluor 633 were detected at  $\lambda = 498$ – $559$  nm,  $\lambda = 568$ – $629$  and  $\lambda = 633$ – $735$  nm, respectively. Super-resolution images of F-actin were acquired using a Nikon N-SIM S microscope, SR HP Apo TIRF 100x 1.49 NA/oil immersion objective and ORCA-Flash 4.0 sCMOS camera, with online deconvolution. Alexa Fluor 488 was excited at  $\lambda = 500$ – $550$  nm, with emitted signals detected at  $\lambda = 570$ – $640$  nm.

### **Intracellular Ca<sup>2+</sup> imaging**

The ratiometric Ca<sup>2+</sup> dye, Fura2 (HelloBio, Catalog# HB0780-1mg), was loaded into islets using 20% pluronic acid dissolved in DMSO (Thermo Fisher Scientific, Cat# P3000MP) at 37°C for 40 mins. For islets treated with GC, 5  $\mu$ M GC (East Coast Bio, Catalog# LA166) was added during Fura2 incubation. Islets were transferred to the heated chamber (34 C) of a Nikon Ti-E microscope coupled to a 10 x / 0.3 NA air objective (Nikon Plan Fluor), allowing simultaneous cell resolution imaging of multiple islets (lateral resolution = 910 nm). A Cairn Research FuraLED system provided excitation at  $\lambda = 340$  nm and  $\lambda = 385$  nm. Emitted signals

were captured at  $\lambda = 470\text{--}550$  nm using a Photometric Delta Evolve EM-CCD. Intracellular  $\text{Ca}^{2+}$  levels were shown as the emission ratio at 340 nm and 385 nm. A number of experiments were repeated using the non-ratiometric  $\text{Ca}^{2+}$  dye Fluo-8 (AAT Bioquest, Catalog# 20494). Confocal excitation was delivered at 470 nm (emission  $\lambda = 500\text{--}550$  nm) by a North 89 LDI Illuminator, CrestOptics V2 X-light spinning disk and 20 x / 0.75 NA air objective (Nikon Plan Apo  $\lambda$ ). Intracellular  $\text{Ca}^{2+}$  levels were quantified as  $F/F_{\min}$  where  $F$  = fluorescence at any given timepoint, and  $F_{\min}$  = mean minimum fluorescence. All experiments were performed in HEPES-bicarbonate buffer was used, containing (in mmol/L) 120 NaCl, 4.8 KCl, 24  $\text{NaHCO}_3$ , 0.5  $\text{Na}_2\text{HPO}_4$ , 5 HEPES, 2.5  $\text{CaCl}_2$ , 1.2  $\text{MgCl}_2$ , and supplemented with 0.5–17 mM D-glucose.

#### **Insulin and glucagon secretion assays**

HEPES-bicarbonate buffer was used for all assays, containing (in mmol/L) 120 NaCl, 4.8 KCl, 24  $\text{NaHCO}_3$ , 0.5  $\text{Na}_2\text{HPO}_4$ , 5 HEPES, 2.5  $\text{CaCl}_2$ , 1.2  $\text{MgCl}_2$  + 0.1% BSA.

For glucagon secretion, batches of 10 islets were pre-incubated in buffer supplemented with:  
1) 10 mM glucose, before incubation with either 10 mM glucose, 0.5 mM glucose or 0.5 mM glucose + 5  $\mu\text{M}$  epinephrine (Sigma-Aldrich, Catalog# E4250) or 5  $\mu\text{M}$  GC for 1 hr at 37°C; or  
2) pre-incubated in 17 mM glucose before incubation with either 17 mM glucose, 2 mM glucose or 2 mM glucose + 5  $\mu\text{M}$  epinephrine. Glucagon released into the supernatant was then measured using either HTRF ultrasensitive assay (Cisbio, Catalog# 62CGLPEG) or Lumit bioluminescent immunoassay (Promega, Catalog# CS3037A06) (26).

For insulin secretion, batches of 10 islets were pre-incubated in buffer supplemented with 3 mM glucose, before sequential incubation in 3 mM glucose, 17 mM glucose and 17 mM glucose + 10 mM KCl or 5  $\mu\text{M}$  GC for 30 mins at 37°C. Insulin was measured using HTRF ultrasensitive assay (Cisbio, Catalog# 62IN2PEG) or Lumit bioluminescent immunoassay (Promega, Catalog# CS3037A01). Total glucagon and insulin were extracted from islets lysed in acid ethanol.



## Image analysis

Ca<sup>2+</sup> imaging:  $\alpha$  cells were identified in an unbiased manner by their characteristic Ca<sup>2+</sup> spiking activity at low glucose, as well as responses to epinephrine, as reported (22; 27). Signal contributions from  $\beta$  cells are unlikely given that they are electrically silent at low glucose and inhibited by epinephrine. The proportion of low glucose-responsive  $\alpha$  cells was calculated as the area occupied by identified  $\alpha$  cells normalized to total islet area. Ca<sup>2+</sup> spike amplitude was calculated for individual cells using  $\Delta F/F_{\min}$ .

Immunostaining: GC, F-actin, G-actin and glucagon were analyzed using corrected total cell fluorescence (CTCF), as previously described. CTCF accounts for the effect of cell size on fluorophore intensity by taking the integrated density and subtracting area of the selected cell x mean background fluorescence (28; 29).  $\alpha$  cell,  $\beta$  cell and  $\delta$  cell area and size were analysed using ImageJ (NIH) Particle Analysis plugin applied to binarized and thresholded images. Linear adjustments to brightness and contrast were applied to representative images, with intensity values maintained between samples to allow cross-comparison.

## Statistics

Statistical details for each experiment are reported in the corresponding figure legend. The n number represents animal, batch of islets or donor. No data were excluded unless the cells displayed a clear non-physiological state (i.e. impaired viability), and all individual data points are reported in the figures. Data normality was assessed using D'Agostino-Pearson test. All analyses were conducted using GraphPad Prism 9.0 software. Pairwise comparisons were made using two-tailed unpaired t test (parametric) or Mann-Whitney test (non-parametric). To assess multiple interactions, one-way or two-way ANOVA were used, adjusted for repeated measures where needed. Post hoc comparisons were made using Bonferroni's, accounting for degrees of freedom. Linear regression was used to assess strength of association between explanatory and dependent variables, with slopes compared using analysis of covariance. Data represent mean  $\pm$  SEM or SD, with individual datapoints shown where possible. Where

a large number of datapoints obscure mean  $\pm$  SEM or SD, violin plots are instead used (showing median and interquartile range).

## **Study approval**

Mouse studies were regulated by the Animals (Scientific Procedures) Act 1986 of the U.K. (Personal Project Licences P2ABC3A83 and PP1778740). Approval was granted by the University of Birmingham's Animal Welfare and Ethical Review Body (AWERB).

Human pancreas sections were obtained from Alberta Diabetes Institute IsletCore (30). Procurement of human pancreases was approved by the Human Research Ethics Board at the University of Alberta (Pro00013094). All donors' families gave informed consent for the use of pancreatic tissue in research. Studies with human tissue were approved by the University of Birmingham Ethics Committee, as well as the National Research Ethics Committee (REC reference 16/NE/0107, Newcastle and North Tyneside, UK). Donor characteristics are reported in Table S1. Anonymized donor IDs can be cross-referenced against the IsletCore database ([www.isletcore.ca](http://www.isletcore.ca)) including information about cold ischemia time, total islet equivalents isolated, tissue purity, insulin content and stimulation index.

## **RESOURCE AVAILABILITY**

All data generated or analyzed during this study are included in the published article (and its online supplementary files). Source data files generated and/or analyzed during the current study are available from the corresponding author upon reasonable request.

## **RESOURCE AVAILABILITY**

Non-commercially available reagents are available from the corresponding author upon reasonable request.

## RESULTS

### Deletion of GC increases basal glucagon secretion during high fat diet

Mice with global GC deletion were used, since: 1) GC is exclusively expressed in  $\alpha$  cells and liver (18; 22); 2) Gcg-Cre lines have variable recombination efficiency and specificity (31); 3) recently reported Gcg-Cre<sup>ERT</sup> knock-in mice require tamoxifen induction (32), which interferes with hepatic triglyceride accumulation and hence GC levels; and 4) two patients with homozygous inactivating mutations in GC have been described (33; 34). The GC<sup>-/-</sup> mice used here are phenotypically well-validated, do not possess detectable GC/Gc expression, and have 50% reduced and 90% reduced 25(OH)D and 1,25(OH)D levels, respectively (22; 25).

GC<sup>-/-</sup> and littermate control GC<sup>+/+</sup> mice were placed on high fat diet (HFD) for up to 12 weeks, with glucose tolerance tested every 4 weeks. The GC<sup>+/+</sup> cohort included some heterozygous (GC<sup>+/-</sup>) animals as controls, since we did not see any differences versus wild-types (GC<sup>+/+</sup>). As expected from our previous studies, glucose tolerance was similar in GC<sup>+/+</sup> and GC<sup>-/-</sup> mice under standard diet (i.e. 0 weeks HFD) (Figure 1A and B). No significant differences were observed in glucose tolerance in GC<sup>+/+</sup> and GC<sup>-/-</sup> mice at 4 weeks, 8 weeks and 12 weeks HFD (Figure 1C-H). Confirming efficacy of the preclinical obesity model, 4-week HFD-fed GC<sup>+/+</sup> and GC<sup>-/-</sup> mice were glucose intolerant versus age-matched controls fed standard chow (Figure 1I). Body weight gain was similar in female and male GC<sup>+/+</sup> and GC<sup>-/-</sup> mice during HFD (Figure 1J and K).

As a similar phenotype was observed in both female and male mice, we combined both sexes for subsequent studies. Plasma glucagon levels were assessed at 0 and 30 mins post-injection of insulin. While glucose levels were lowered to a similar extent in GC<sup>+/+</sup> and GC<sup>-/-</sup> mice (Figure 1L), basal fasted glucagon secretion was significantly (2-fold) elevated in GC<sup>-/-</sup> mice after 4 weeks of HFD (Figure 1M-O). Glucagon:glucose ratios, calculated using measures from the same animal, provided further evidence of dysregulated basal but not stimulated glucagon secretion (Figure 1M and P).

In summary, GC<sup>-/-</sup> mice are glucose tolerant during HFD, but display elevated basal glucagon levels, indicative of dysregulated  $\alpha$  cell function.

#### **HFD GC<sup>-/-</sup> mice have aberrant $\alpha$ -, $\beta$ - and $\delta$ -cell morphology**

Pancreata isolated from HFD-fed GC<sup>+/+</sup> mice showed a 2-fold increase in GC protein levels versus standard chow (SC) controls (Figure 2A and B). GC protein was undetectable in pancreata from HFD-fed GC<sup>-/-</sup> mice, further demonstrating the reliability of the antibody and immunostaining approach used (22) (Figure 2A and B). We have previously shown that pancreata from SC-fed GC<sup>-/-</sup> mice possess decreased  $\alpha$  cell mass and  $\alpha$  cell size (22). We thus performed high resolution morphometric analysis in pancreata from HFD-fed mice.

HFD feeding itself did not affect islet area occupied by  $\alpha$  cells, nor  $\alpha$  cell size, as compared to age-matched SC controls (Figure 2C-E). However, a large reduction in  $\alpha$  cell size was observed in HFD-fed GC<sup>-/-</sup> mice versus GC<sup>+/+</sup> littermates (Figure 2C-E). By contrast to its effects on  $\alpha$  cells, HFD increased  $\beta$  cell size in GC<sup>+/+</sup>, with a further increase detected in GC<sup>-/-</sup> islets (Figure 2C, F and G). Analysis of  $\delta$  cells revealed a HFD-induced increase in their proportion, a change that was partly reversed by deletion of GC (Figure 2H-J).

In summary, these data suggest that, during HFD, GC restrains  $\beta$  cell size, while promoting  $\alpha$  cell size and  $\delta$  cell expansion to support normal plasticity.

#### **Glucagon secretion and $\alpha$ cell Ca<sup>2+</sup> responses are impaired in HFD GC<sup>-/-</sup> islets**

Islets were isolated from HFD-fed GC<sup>+/+</sup> and GC<sup>-/-</sup> mice and their age-matched standard chow controls for detailed in vitro analyses. As reported previously (22), SC GC<sup>-/-</sup> islets presented with impaired low glucose- and low glucose + epinephrine-stimulated glucagon secretion versus GC<sup>+/+</sup> littermates (Figure 3A). Similar impairments were detected for HFD, although responses to epinephrine remained intact, suggesting that the defect is upstream of the exocytotic machinery (Figure 3A). At glucose concentration sub-maximal for alpha cell function (i.e. 2 mM), glucagon secretion still tended to be reduced in HFD GC<sup>-/-</sup> islets (Figure

3B). Glucose-stimulated insulin secretion tended to be increased in SC GC<sup>-/-</sup> islets and this trend became significant during HFD (Figure 3C). A tendency toward increased basal glucagon secretion was also noted in HFD GC<sup>-/-</sup> islets (Figure 3B), which might partly explain the increased insulin secretion, since glucagon is insulinotropic when beta cells are active (35). No significant differences in total glucagon or insulin content could be detected between GC<sup>-/-</sup> islets and GC<sup>+/+</sup> controls (Figure 3 D and E).

Given the apparent changes in glucagon and insulin secretion, we next investigated upstream Ca<sup>2+</sup> fluxes, with  $\alpha$  cells identified by their characteristic responses to low glucose (0.5 mM) as well as epinephrine (27). Confirming our previous findings, proportion active  $\alpha$  cells (i.e. % cells displaying Ca<sup>2+</sup> spikes; a measure of recruitment into Ca<sup>2+</sup> activity) was decreased in SC GC<sup>-/-</sup> islets (Figure 3F-I). By contrast to our previous results, we also observed a significant decrease in Ca<sup>2+</sup> amplitude in SC GC<sup>-/-</sup> islets (Figure 3G-I). The most likely explanation for this discrepancy is the relatively advanced age of the SC mice used in the study here, which were age-matched with those receiving HFD, and suggests that age might exacerbate the in vitro phenotype following GC deletion. Nonetheless, HFD decreased both the proportion of active  $\alpha$  cells, as well as the amplitude of their Ca<sup>2+</sup> spikes (Figure 3F-I). The effect of HFD on Ca<sup>2+</sup> spike amplitude, but not proportion active  $\alpha$  cells, was exacerbated following loss of GC (Figure 3F-I) (Supplementary Movies 1 and 2). Ca<sup>2+</sup> imaging results were validated using a second Ca<sup>2+</sup> probe (Fluo8), confocal microscopy and a higher magnification objective (Figure 3J-K) (Supplementary Movies 3 and 4).

### **GC-dependent actin cytoskeleton remodelling occurs during HFD**

During stimulation, the F-actin cytoskeleton undergoes rearrangement to facilitate exocytosis of hormone vesicles (36-38). In line with the actin-scavenging function of GC, we previously showed that F-actin density was increased in GC<sup>-/-</sup> islets, leading to changes in glucagon granule morphology and distribution, suggestive of sequestration and trapping (22). Directly implicating the F-actin cytoskeleton in glucagon release, incubation of GC<sup>-/-</sup> islets with

Latrunculin B was able to restore function (22). We therefore investigated whether restoration of GC level and ergo F-actin cytoskeletal structure might rescue the phenotype of HFD GC<sup>-/-</sup> islets. Following acute (10 mins) stimulation with low glucose, F-actin density was decreased in GC<sup>-/-</sup> islets but unchanged in islets from GC<sup>+/+</sup> islets (Figure 4A-C). F-actin remained low in GC<sup>-/-</sup> islets after chronic (60 mins) stimulation, but was increased ~2-fold in GC<sup>+/+</sup> islets (Figure 4A-C).

As we previously showed (22), deletion of GC from standard chow islets led to increased F-actin density, concomitant with a decrease in G-actin monomers, presumably due to their involvement in forming polymerized actin (Figure 4D-F). On the other hand, F-actin density and fiber thickness increased by almost 3-fold in HFD GC<sup>+/+</sup> islets (Figure 4D-F). Unexpectedly, given its actin scavenging function, deletion of GC led to a decrease in F-actin density in HFD GC<sup>-/-</sup> islets versus GC<sup>+/+</sup> controls (Figure 4D-E). By contrast, monomeric G-actin was increased in HFD GC<sup>-/-</sup> islets, suggesting that G-actin is sequestered away from sites of F-actin polymerization following deletion of GC (Figure 4D-F). In all cases, changes in F-actin and G-actin were detected throughout the islet (Figure 4E and F) as well as in individual  $\alpha$  cells (Figure 4G and H) and  $\beta$  cells (Figure 4I and J), suggesting that glucagon granule-resident GC acts in a paracrine manner to influence cytoskeletal structure throughout the islet i.e. by severing and depolymerizing F-actin into G-actin (22; 38).

### **GC supplementation restores F-actin cytoskeletal structure and glucagon release**

We next investigated whether exogenous GC could modify F-actin levels in GC<sup>-/-</sup> islets to restore  $\alpha$  cell activity. Using a published RNA-seq dataset (19), transcripts for the endocytic receptors responsible for GC uptake, megalin (*Lrp2*) and cubilin (*Cubn*) (14; 39-41), were found to be expressed in purified  $\alpha$  cells at a similar level to the gastric inhibitory polypeptide receptor (*Gipr*) (normalized expression:  $8.9 \pm 5.3$  versus  $9.7 \pm 3.4$  versus  $8.0 \pm 7.0$  for *Lrp2* versus *Cubn* versus *Gipr*, respectively) (taken from (GSE76017)). As expected from this, GC levels could be restored in HFD GC<sup>-/-</sup> islets following incubation with exogenous protein (Figure

5A-C). Confirming the directionality of F-actin changes, treatment of HFD GC<sup>-/-</sup> islets with GC restored F-actin levels to wild-type levels (Figure 5D), as seen throughout the islet as well as in individual  $\alpha$  cells (Figure 5C-E).

As expected, low glucose (G0.5)-stimulated glucagon secretion was impaired in HFD GC<sup>-/-</sup> islets (22). Pertinently, application of GC restored normal glucagon secretion in HFD GC<sup>-/-</sup> islets, without influencing the function of HFD GC<sup>+/+</sup> islets (Figure 5F). The effects of GC on glucagon secretion were not associated with increases in intracellular Ca<sup>2+</sup> concentration, which was slightly but significantly decreased in GC-treated islets (Figure 5G and H). Reflecting either the lowered glucagon tone or decreased F-actin in GC<sup>-/-</sup> islets, insulin secretion failed to shut off at low glucose (0.5 mM) (Figure 5I), an effect remarkably similar to that reported when the small GTPase and actin polymerizer, RhoA, is inhibited in  $\alpha$  cells (42). GC treatment was unable to restore this defect or influence basal insulin levels in either GC<sup>+/+</sup> or GC<sup>-/-</sup> islets (Figure 5I). By contrast, GC treatment led to a large (~ 10-fold) amplification of glucose-stimulated insulin secretion, with a greater effect in HFD GC<sup>-/-</sup> islets (Figure 5J)

Finally, as a proof of principle, we were able to show that GC could be supplemented in human islets, leading to increases in glucagon granule area as well as F-actin density (Figure 5K-M), visualized at ~110 nm resolution using structured illumination microscopy.

#### **GC expression is decreased in islets of T2D donors**

In pancreas sections from non-diabetic (ND) donors, GC expression was only present in  $\alpha$  cells, as expected (18; 22; 43) (Figure 6A). While a similar staining pattern was observed in pancreas sections from T2D donors, GC expression levels were markedly (~ 2-fold) reduced (Figure 6A). Some inter-individual variability was observed, but reduced GC expression appeared to be a remarkably consistent feature of T2D (Figure 6B and C). Reflecting findings in HFD mice, analysis of individual  $\alpha$  cells in T2D donors revealed a decrease in cell size (Figure 6D and E). While proportion of islet area occupied by  $\delta$  cells was unchanged during T2D,  $\delta$  cell size was slightly but significantly reduced (Figure 6F-I).

Linear regression showed a strong correlation between GC and glucagon expression in  $\alpha$  cells from donors without diabetes (Figure 6J). Whilst a significant linear correlation was also detected for individuals with T2D, the strength of correlation was much lower (Figure 6K), consistent with the reported decrease in GC expression (Figure 6B), as well  $\alpha$  cell glucagon expression (Figure 6L). As expected from this, the regression slopes were significantly different between ND and T2D samples ( $P < 0.001$ ). Together, these analyses show that glucagon expression co-varies with GC expression and that this relationship is partly lost during T2D.



## DISCUSSION

In the present study, we show that deletion of GC in HFD-fed animals leads to basal hyperglucagonemia and impaired low glucose-stimulated glucagon secretion. These secretory defects are associated with changes in  $\text{Ca}^{2+}$  fluxes,  $\alpha$  cell,  $\beta$  cell and  $\delta$  cell size and mass, as well as F-actin and G-actin abundance.  $\alpha$  cell function can be restored in  $\text{GC}^{-/-}$  islets by using exogenous GC, which is taken up into cells following culture. Lastly, islets from donors with T2D show decreases in GC expression, with concomitant changes in  $\alpha$  cell and  $\delta$  cell size and mass. Together, these results expand our previous findings on GC by revealing its regulatory role in glucagon secretion during metabolic stress, and further suggest that GC is a pivotal component of the  $\alpha$  cell phenotype in health and disease. While GC is a signature gene expressed in  $\alpha$  cells, the current study shows that  $\alpha$  cells also have the potential to acquire GC via megalin-mediated endocytosis. This raises the possibility that circulating levels of GC may also contribute to  $\alpha$  cell GC-actin dynamics and phenotype.

*In vivo* metabolic phenotyping demonstrated that  $\text{GC}^{+/+}$  and  $\text{GC}^{-/-}$  mice possess similar glucose excursion curves in response to intraperitoneal glucose injection. However, basal plasma glucagon concentrations were consistently raised in  $\text{GC}^{-/-}$  mice, in line with a tendency toward elevated glucagon secretion from isolated islets at 17 mM glucose, which would be expected to increase hepatic glucose output. One possible explanation for the apparently normal glucose homeostasis is that the increase in glucagon levels is not sufficient to influence insulin counter-regulation, or might even act to prime  $\beta$  cells for insulin secretion (44; 45). Alternatively, recent studies have shown that *Gc* is upregulated in de-differentiated  $\beta$  cells and deletion of *GC* increases glucose-stimulated insulin secretion and liver insulin sensitivity at 12 weeks HFD (24). In any case, these data show that HFD-induced basal hyperglucagonemia (46) is further aggravated following GC deletion. We were unable to reliably detect significant increases in *in vitro* insulin secretion or  $\beta$  cell function at 4-8 weeks HFD, arguing against this possibility here, although we concede that clamp studies are needed to properly assess this.

Moreover, GC expression was variably upregulated in  $\beta$  cells, remaining much lower than the levels seen in  $\alpha$  cells.

Plasma glucagon levels, stimulated by insulin injection, were almost identical in HFD-fed GC<sup>+/+</sup> and GC<sup>-/-</sup> mice, despite impaired glucagon release from isolated islets incubated in low (0.5 mM) glucose. We found, however, that the effect of GC deletion was milder in islets exposed to sub-maximal (2 mM) glucose concentration, which would be closer to that achieved in vivo. Together, these data suggest that GC is relatively more important in alpha cells operating close to their functional ceiling, with the caveat that in vitro glucagon secretion assays might be less sensitive at 2 mM glucose due to the relatively smaller magnitude change. Along similar lines, HFD-fed GC<sup>-/-</sup> mice presented with basal hyperglucagonemia at blood glucose concentrations ~ 10-11 mmol/L, whilst in isolated islets basal glucagon secretion was similar in GC<sup>-/-</sup> and GC<sup>+/+</sup> mice at high glucose. One explanation for this discrepancy might lie in the finding that glucose-stimulated insulin secretion was almost 2-fold increased in HFD-fed GC<sup>-/-</sup> islets. In vivo, relative hyperinsulinemia would be expected to drive hyperglucagonemia to maintain blood glucose levels, which were not different between HFD-fed GC<sup>+/+</sup> and GC<sup>-/-</sup> mice. Another explanation might lie in the changes in  $\alpha$  cell morphology observed in pancreas sections taken from HFD-fed GC<sup>-/-</sup> animals. A decrease in  $\alpha$  cell size might lead to an increase in  $\alpha$  cell membrane juxtaposed with the islet capillaries, favoring release of glucagon into the circulation.

During standard diet, we showed that loss of GC leads to a large increase in the density of the F-actin cytoskeleton (and concomitant decrease in G-actin), acting as a physical barrier against exocytosis of glucagon granules during low glucose stimulation (22). Changes in the F-actin and G-actin cytoskeleton occur throughout the islet, since ~ 50% of GC is present in glucagon granules and can readily be taken up by neighboring cells by endocytosis, as shown here following application of exogenous GC. Following 4-8 weeks HFD, F-actin density was increased almost 2-fold in GC<sup>+/+</sup> islets. On a background of metabolic stress, deletion of GC did not further increase F-actin density. In fact, HFD GC<sup>-/-</sup> islets showed a surprising reduction

in F-actin density, contrary to our previous findings in standard diet islets (22). A similar decrease in F-actin density was seen in GC<sup>-/-</sup> islets stimulated with low glucose for 60 mins. Notably, treatment with exogenous GC replenished intracellular GC and F-actin levels in HFD GC<sup>-/-</sup> islets, confirming that GC acts to increase F-actin density during metabolic stress. Given that GC is a potent actin scavenger, what might be the mechanisms involved in this apparent decrease in F-actin? A likely mechanism revolves around G-actin, which was virtually undetectable in HFD GC<sup>-/-</sup> islets. Without G-actin to supply monomers, polymerized F-actin cannot be formed. Indeed, previous reports by us have shown a similar decrease in F-actin in trophoblasts depleted for GC, which was associated with an increase in G-actin monomers in the nucleus where they are unavailable for assembly into polymerized F-actin (39). Another mechanism might be a large compensatory upregulation in gelsolin, which severs F-actin into G-actin (36; 47), although we would expect this to be associated with an increase in G-actin levels.

Kuo *et al.* recently reported that GC<sup>-/-</sup> islets show an insulin signaling/sensitivity defect, but exhibit a normal glucagon phenotype under both standard diet and high fat diet conditions (24). Since our studies used islets from animals on 4 and 8 week HFD, we cannot exclude that glucagon secretion in GC<sup>-/-</sup> animals/islets normalizes in line with improved  $\beta$  cell function at 12 weeks, the feeding period used by Kuo *et al.* We also used a different GC knockout mouse line, which might give rise to a different phenotype. However, it should be noted that these animals are well-validated by multiple groups and show complete loss of GC in  $\alpha$  cells and the liver, undetectable circulating GC based upon LC-MS, and a 90% reduction in circulating 25(OH)D in homozygotes (22; 25). Suggesting that GC plays a critical role in  $\alpha$  cell biology: 1) GC is an  $\alpha$  cell signature gene; 2) GC protein expression is upregulated during HFD, remaining 10-100-fold higher than that in  $\beta$  cells; and 3) defects in  $\alpha$  cell function have a clear mechanistic basis, including changes in cell morphology, cell mass, cytoskeletal structure and ionic fluxes, shown also by recent Patch-seq studies (8). Nonetheless, these studies together posit that, depending on duration of metabolic stress, effects of GC deletion

(and GC supplementation) can be seen on both the insulin and glucagon axes. Further studies using conditional GC deletion in  $\alpha$  cells and  $\beta$  cells are warranted.

Studies in human donor pancreas sections revealed that GC and glucagon expression are positively associated, with levels co-varying across hundreds of individual cells examined, a relationship that was lost during T2D. Mechanistically, this observation likely reflects changes in the alpha cell transcription factor network, since GC possesses cell type-selective open chromatin regions (18). Ultimately, however, altered gene regulation must impact functional protein targets, and our in vitro findings support the notion that the disrupted relationship between GC and glucagon might contribute to impaired glucagon secretion during T2D. Further studies are warranted in isolated human islets to investigate the effects of silencing GC on glucagon expression and secretion in  $\alpha$  cells.

Changes in the actin cytoskeleton could be rescued using exogenous GC. In the kidney, GC-bound 25(OH)D is taken up by facilitated endocytotic uptake via the megalin-cubulin complex (14; 41; 48), where liberated 25(OH)D is then converted to 1,25(OH)<sub>2</sub>D. Immunostaining clearly showed dose-dependent uptake of GC into islets, demonstrating that similar transport mechanisms also exist in the pancreas, as suggested by published RNA-seq data (49). These data suggest that, unusually, decreases in expression of a key cell signature gene can be offset by supplementing its protein product and warrant further investigation of the uptake mechanisms involved. While these results point to GC as a therapeutic target, caution should be extended due to opposing effects of GC on both the  $\alpha$  cell and  $\beta$  cell compartments (24). However, it should be noted that high glucose levels have been shown to inhibit megalin-mediated endocytosis, which might differentially affect GC uptake into  $\alpha$  cells and  $\beta$  cells (50). Moreover, molecular addresses such as V1BR could be used to target GC specifically to  $\alpha$  cells (51-53). In any case, we envisage that GC administration during type 2 diabetes could maintain  $\alpha$  cell function, whilst restraining  $\beta$  cell proliferation and hyperinsulinemia, known to drive insulin resistance (54; 55). Our data in human pancreas sections supports a reduction

in GC during type 2 diabetes, lending further weight to this argument. Nonetheless, careful preclinical studies in mice at various timepoints are required to assess this.

There are a number of limitations in the present study. Firstly, we used a well-phenotyped global GC<sup>-/-</sup> mouse model in which GC is undetectable in the circulation. Whilst GC<sup>-/-</sup> mice are vitamin D sufficient (22), we cannot exclude that loss of circulating GC influences  $\alpha$  cell phenotype and function. In the future, it will be worthwhile conditionally deleting GC in the  $\alpha$  cell or liver to explore the role of circulating GC in  $\alpha$  cell and more widely islet function. Secondly, we decided to investigate HFD at 4 and 8 weeks, since longer feeding periods did not lead to further changes in glucose tolerance. In any case, this length of HFD allowed  $\alpha$  cell function to be determined without any confounding affects caused by GC upregulation in the  $\beta$  cell compartment, as shown by our immunohistochemical analyses. Thirdly, the mild in vivo phenotype seen in HFD-fed GC<sup>-/-</sup> mice might reflect compensation, especially since the gene was (presumably) deleted during development. Finally, whilst GC supplementation increased glucagon granule area/density in human  $\alpha$  cells, it should be noted that the decrease in GC levels seen in samples from T2D donors is associative and might be a consequence rather than a cause of changes in  $\alpha$  cell morphology and function.

In summary, we show that  $\alpha$  cells lacking GC fail to adapt properly to metabolic stress, displaying a range of defects leading to impaired basal and low glucose-stimulated glucagon release. Given its role under both normal and obesogenic conditions, GC should thus be considered as a key regulator of  $\alpha$  cell function and glucagon secretion.

499 **FUNDING**

500 D.J.H. was supported by MRC (MR/S025618/1) and Diabetes UK (17/0005681) Project  
501 Grants, as well as a UKRI ERC Frontier Research Guarantee Grant (EP/X026833/1). This  
502 project has received funding from the European Research Council (ERC) under the European  
503 Union's Horizon 2020 research and innovation programme (Starting Grant 715884 to D.J.H.).  
504 L.J.B.B. was supported by a Sir Henry Wellcome Postdoctoral Fellowship (Wellcome Trust,  
505 201325/Z/16/Z) and a Junior Research Fellowship from Trinity College, Oxford. The research  
506 was funded by the National Institute for Health Research (NIHR) Oxford Biomedical Research  
507 Centre (BRC). The views expressed are those of the author(s) and not necessarily those of  
508 the NHS, the NIHR or the Department of Health. Human pancreas sections were provided by  
509 the Alberta Diabetes Institute IsletCore at the University of Alberta in Edmonton  
510 (<http://www.bcell.org/adi-isletcore.html>) with the assistance of the Human Organ Procurement  
511 and Exchange (HOPE) program, Trillium Gift of Life Network (TGLN) and other Canadian  
512 organ procurement organizations. The funders had no role in study design, data collection,  
513 data analysis, interpretation or writing of the paper.

514 **DUALITY OF INTEREST**

515 D.J.H. receives licensing revenue from Celtarys Research. K.V., M.H. and D.J.H. are named  
516 on a patent application regarding use of GC-globulin as an anti-diabetic therapy.

517 **AUTHOR CONTRIBUTIONS**

518 K.V., D.N., J.A., A.H., F.C., L.J.B.B. and S.H. performed experiments and analyzed data.  
519 D.J.H. and M.H. conceived and designed the studies. D.J.H. and M.H. supervised the studies.  
520 D.J.H., M.H. and K.V. wrote the paper with input from all authors. M.H. and D.J.H are the  
521 guarantors of this work, had full access to all the data, and take full responsibility for the  
522 integrity of data and the accuracy of data analysis.

523 **ACKNOWLEDGEMENTS**

524 We thank Prof Patrick E. MacDonald and Dr Jocelyn Manning Fox (Alberta Diabetes Institute  
525 IsletCore at the University of Alberta in Edmonton) for provision of human pancreas sections.

526

## REFERENCES

1. D'Alessio D: The role of dysregulated glucagon secretion in type 2 diabetes. *Diabetes, Obesity and Metabolism* 2011;13:126-132
2. McCrimmon RJ, Sherwin RS: Hypoglycemia in Type 1 Diabetes. *Diabetes* 2010;59:2333-2339
3. Dean ED, Li M, Prasad N, Wisniewski SN, Von Deylen A, Spaeth J, Maddison L, Botros A, Sedgeman LR, Bozadjieva N, Ilkayeva O, Coldren A, Poffenberger G, Shostak A, Semich MC, Aamodt KI, Phillips N, Yan H, Bernal-Mizrachi E, Corbin JD, Vickers KC, Levy SE, Dai C, Newgard C, Gu W, Stein R, Chen W, Powers AC: Interrupted Glucagon Signaling Reveals Hepatic  $\alpha$  Cell Axis and Role for L-Glutamine in  $\alpha$  Cell Proliferation. *Cell Metabolism* 2017;25:1362-1373.e1365
4. Gromada J, Chabosse P, Rutter GA: The  $\alpha$ -cell in diabetes mellitus. *Nature Reviews Endocrinology* 2018;14:694-704
5. Zhang Q, Ramracheya R, Lahmann C, Tarasov A, Bengtsson M, Braha O, Braun M, Brereton M, Collins S, Galvanovskis J, Gonzalez A, Groschner LN, Rorsman NJ, Salehi A, Travers ME, Walker JN, Gloyn AL, Gribble F, Johnson PR, Reimann F, Ashcroft FM, Rorsman P: Role of KATP channels in glucose-regulated glucagon secretion and impaired counterregulation in type 2 diabetes. *Cell Metab* 2013;18:871-882
6. Vieira E, Salehi A, Gylfe E: Glucose inhibits glucagon secretion by a direct effect on mouse pancreatic alpha cells. *Diabetologia* 2007;50:370-379
7. Omar-Hmeadi M, Lund P-E, Gandasi NR, Tengholm A, Barg S: Paracrine control of  $\alpha$ -cell glucagon exocytosis is compromised in human type-2 diabetes. *Nature Communications* 2020;11
8. Dai X-Q, Camunas-Soler J, Briant LJB, Santos Td, Spigelman AF, Walker EM, Arrojo e Drigo R, Bautista A, Jones RC, Lyon J, Nie A, Smith N, Fox JEM, Kim SK, Rorsman P, Stein RW, Quake SR, MacDonald PE: Heterogenous impairment of  $\alpha$ -cell function in type 2 diabetes is linked to cell maturation state. 2021;



554 9. Lee Y, Wang MY, Du XQ, Charron MJ, Unger RH: Glucagon receptor knockout prevents  
555 insulin-deficient type 1 diabetes in mice. *Diabetes* 2011;60:391-397

556 10. Okamoto H, Cavino K, Na E, Krumm E, Kim SY, Cheng X, Murphy AJ, Yancopoulos GD,  
557 Gromada J: Glucagon receptor inhibition normalizes blood glucose in severe insulin-resistant  
558 mice. *Proceedings of the National Academy of Sciences* 2017;114:2753-2758

559 11. Brand CL, Rolin B, Jørgensen PN, Svendsen I, Kristensen JS, Holst JJ:  
560 Immunoneutralization of endogenous glucagon with monoclonal glucagon antibody  
561 normalizes hyperglycaemia in moderately streptozotocin-diabetic rats. *Diabetologia*  
562 1994;37:985-993

563 12. Sorensen H, Brand CL, Neschen S, Holst JJ, Fosgerau K, Nishimura E, Shulman GI:  
564 Immunoneutralization of Endogenous Glucagon Reduces Hepatic Glucose Output and  
565 Improves Long-Term Glycemic Control in Diabetic ob/ob Mice. *Diabetes* 2006;55:2843-2848

566 13. Daiger SP, Schanfield MS, Cavalli-Sforza LL: Group-specific component (Gc) proteins  
567 bind vitamin D and 25-hydroxyvitamin D. *Proc Natl Acad Sci U S A* 1975;72:2076-2080

568 14. Bouillon R, Schuit F, Antonio L, Rastinejad F: Vitamin D Binding Protein: A Historic  
569 Overview. *Frontiers in Endocrinology* 2020;10

570 15. McLeod JF, Kowalski MA, Haddad JG, Jr.: Interactions among serum vitamin D binding  
571 protein, monomeric actin, profilin, and profilactin. *J Biol Chem* 1989;264:1260-1267

572 16. Harper KD, McLeod JF, Kowalski MA, Haddad JG: Vitamin D binding protein sequesters  
573 monomeric actin in the circulation of the rat. *Journal of Clinical Investigation* 1987;79:1365-  
574 1370

575 17. Bikle Daniel D: Vitamin D Metabolism, Mechanism of Action, and Clinical Applications.  
576 *Chemistry & Biology* 2014;21:319-329

577 18. Ackermann AM, Wang Z, Schug J, Naji A, Kaestner KH: Integration of ATAC-seq and  
578 RNA-seq identifies human alpha cell and beta cell signature genes. *Mol Metab* 2016;5:233-  
579 244

580 19. Adriaenssens AE, Svendsen B, Lam BYH, Yeo GSH, Holst JJ, Reimann F, Gribble FM:  
581 Transcriptomic profiling of pancreatic alpha, beta and delta cell populations identifies delta  
582 cells as a principal target for ghrelin in mouse islets. *Diabetologia* 2016;59:2156-2165

583 20. Akerman I, Tu Z, Beucher A, Rolando DMY, Sauty-Colace C, Benazra M, Nakic N, Yang  
584 J, Wang H, Pasquali L, Moran I, Garcia-Hurtado J, Castro N, Gonzalez-Franco R, Stewart AF,  
585 Bonner C, Piemonti L, Berney T, Groop L, Kerr-Conte J, Pattou F, Argmann C, Schadt E,  
586 Ravassard P, Ferrer J: Human Pancreatic beta Cell lncRNAs Control Cell-Specific Regulatory  
587 Networks. *Cell Metab* 2017;25:400-411

588 21. Lu L, Bennett DA, Millwood IY, Parish S, McCarthy MI, Mahajan A, Lin X, Bragg F, Guo  
589 Y, Holmes MV, Afzal S, Nordestgaard BG, Bian Z, Hill M, Walters RG, Li L, Chen Z, Clarke R:  
590 Association of vitamin D with risk of type 2 diabetes: A Mendelian randomisation study in  
591 European and Chinese adults. *PLoS Med* 2018;15:e1002566

592 22. Vilorio K, Nasteska D, Briant LJB, Heising S, Larner DP, Fine NHF, Ashford FB, da Silva  
593 Xavier G, Ramos MJ, Hasib A, Cuzzo F, Manning Fox JE, MacDonald PE, Akerman I, Lavery  
594 GG, Flaxman C, Morgan NG, Richardson SJ, Hewison M, Hodson DJ: Vitamin-D-Binding  
595 Protein Contributes to the Maintenance of  $\alpha$  Cell Function and Glucagon Secretion. *Cell*  
596 *Reports* 2020;31

597 23. Vilorio K, Hewison M, Hodson DJ: Vitamin D binding protein/GC-globulin: A novel regulator  
598 of alpha cell function and glucagon secretion. *The Journal of Physiology* 2021;

599 24. Kuo T, Damle M, González BJ, Egli D, Lazar MA, Accili D: Induction of  $\alpha$  cell-restricted  
600 Gc in dedifferentiating  $\beta$  cells contributes to stress-induced  $\beta$  cell dysfunction. *JCI Insight*  
601 2019;4

602 25. Safadi FF, Thornton P, Magiera H, Hollis BW, Gentile M, Haddad JG, Liebhaber SA,  
603 Cooke NE: Osteopathy and resistance to vitamin D toxicity in mice null for vitamin D binding  
604 protein. *J Clin Invest* 1999;103:239-251

605 26. El K, Gray SM, Capozzi ME, Knuth ER, Jin E, Svendsen B, Clifford A, Brown JL, Encisco  
606 SE, Chazotte BM, Sloop KW, Nunez DJ, Merrins MJ, D'Alessio DA, Campbell JE: GIP

607 mediates the incretin effect and glucose tolerance by dual actions on  $\alpha$  cells and  $\beta$  cells.  
608 Science Advances 2021;7

609 27. Hamilton A, Zhang Q, Salehi A, Willems M, Knudsen JG, Ringgaard AK, Chapman CE,  
610 Gonzalez-Alvarez A, Surdo NC, Zaccolo M, Basco D, Johnson PRV, Ramracheya R, Rutter  
611 GA, Galione A, Rorsman P, Tarasov AI: Adrenaline Stimulates Glucagon Secretion by Tpc2-  
612 Dependent  $\text{Ca}^{2+}$  Mobilization From Acidic Stores in Pancreatic  $\alpha$ -Cells. Diabetes  
613 2018;67:1128-1139

614 28. Gavet O, Pines J: Progressive activation of CyclinB1-Cdk1 coordinates entry to mitosis.  
615 Dev Cell 2010;18:533-543

616 29. McCloy RA, Rogers S, Caldon CE, Lorca T, Castro A, Burgess A: Partial inhibition of Cdk1  
617 in G 2 phase overrides the SAC and decouples mitotic events. Cell Cycle 2014;13:1400-1412

618 30. Lyon J, Manning Fox JE, Spigelman AF, Kim R, Smith N, O'Gorman D, Kin T, Shapiro AM,  
619 Rajotte RV, MacDonald PE: Research-Focused Isolation of Human Islets From Donors With  
620 and Without Diabetes at the Alberta Diabetes Institute IsletCore. Endocrinology 2016;157:560-  
621 569

622 31. da Silva Xavier G, Hodson DJ: Mouse models of peripheral metabolic disease. Best  
623 Practice & Research Clinical Endocrinology & Metabolism 2018;

624 32. Ackermann AM, Zhang J, Heller A, Briker A, Kaestner KH: High-fidelity Glucagon-CreER  
625 mouse line generated by CRISPR-Cas9 assisted gene targeting. Mol Metab 2017;6:236-244

626 33. Henderson CM, Fink SL, Bassyouni H, Argiropoulos B, Brown L, Laha TJ, Jackson KJ,  
627 Lewkonja R, Ferreira P, Hoofnagle AN, Marcadier JL: Vitamin D–Binding Protein Deficiency  
628 and Homozygous Deletion of the GC Gene. New England Journal of Medicine 2019;380:1150-  
629 1157

630 34. Banerjee RR, Spence T, Frank SJ, Pandian R, Hoofnagle AN, Argiropoulos B, Marcadier  
631 JL: Very Low Vitamin D in a Patient With a Novel Pathogenic Variant in the GC Gene That  
632 Encodes Vitamin D-Binding Protein. J Endocr Soc 2021;5:bvab104

633 35. Capozzi ME, Wait JB, Koech J, Gordon AN, Coch RW, Svendsen B, Finan B, D'Alessio  
634 DA, Campbell JE: Glucagon lowers glycemia when beta-cells are active. JCI Insight 2019;5

36. Tomas A, Yermen B, Min L, Pessin JE, Halban PA: Regulation of pancreatic beta-cell insulin secretion by actin cytoskeleton remodelling: role of gelsolin and cooperation with the MAPK signalling pathway. *J Cell Sci* 2006;119:2156-2167
37. Hoboth P, Muller A, Ivanova A, Mziaut H, Dehghany J, Sonmez A, Lachnit M, Meyer-Hermann M, Kalaidzidis Y, Solimena M: Aged insulin granules display reduced microtubule-dependent mobility and are disposed within actin-positive multigranular bodies. *Proc Natl Acad Sci U S A* 2015;112:E667-676
38. Kalwat MA, Thurmond DC: Signaling mechanisms of glucose-induced F-actin remodeling in pancreatic islet  $\beta$  cells. *Experimental & Molecular Medicine* 2013;45:e37-e37
39. Ganguly A, Tamblyn JA, Shattock A, Joseph A, Lerner DP, Jenkinson C, Gupta J, Gross SR, Hewison M: Trophoblast uptake of DBP regulates intracellular actin and promotes matrix invasion. *J Endocrinol* 2021;249:43-55
40. Rowling MJ, Kemmis CM, Taffany DA, Welsh J: Megalin-mediated endocytosis of vitamin D binding protein correlates with 25-hydroxycholecalciferol actions in human mammary cells. *J Nutr* 2006;136:2754-2759
41. Christensen EI, Birn H: Megalin and cubilin: multifunctional endocytic receptors. *Nature Reviews Molecular Cell Biology* 2002;3:258-267
42. Ng XW, Chung YH, Asadi F, Kong C, Ustione A, Piston DW: RhoA as a Signaling Hub Controlling Glucagon Secretion from Pancreatic  $\alpha$ -Cells. *Diabetes* 2022;
43. Lam CJ, Chatterjee A, Shen E, Cox AR, Kushner JA: Low-Level Insulin Content Within Abundant Non- $\beta$  Islet Endocrine Cells in Long-standing Type 1 Diabetes. *Diabetes* 2019;68:598-608
44. Capozzi ME, Svendsen B, Encisco SE, Lewandowski SL, Martin MD, Lin H, Jaffe JL, Coch RW, Haldeman JM, MacDonald PE, Merrins MJ, D'Alessio DA, Campbell JE: beta Cell tone is defined by proglucagon peptides through cAMP signaling. *JCI Insight* 2019;4
45. El K, Capozzi ME, Campbell JE: Repositioning the Alpha Cell in Postprandial Metabolism. *Endocrinology* 2020;161

662 46. Kellard JA, Rorsman NJG, Hill TG, Armour SL, van der Bunt M, Rorsman P, Knudsen JG,  
663 Briant LJB: Reduced somatostatin signalling leads to hypersecretion of glucagon in mice fed  
664 a high fat diet. *Molecular Metabolism* 2020;

665 47. Nelson TY, Boyd AE, 3rd: Gelsolin, a Ca<sup>2+</sup>-dependent actin-binding protein in a hamster  
666 insulin-secreting cell line. *Journal of Clinical Investigation* 1985;75:1015-1022

667 48. Nykjaer A, Dragun D, Walther D, Vorum H, Jacobsen C, Herz J, Melsen F, Christensen  
668 EI, Willnow TE: An Endocytic Pathway Essential for Renal Uptake and Activation of the Steroid  
669 25-(OH) Vitamin D3. *Cell* 1999;96:507-515

670 49. Blodgett DM, Nowosielska A, Afik S, Pechhold S, Cura AJ, Kennedy NJ, Kim S, Kucukural  
671 A, Davis RJ, Kent SC, Greiner DL, Garber MG, Harlan DM, dilorio P: Novel Observations  
672 From Next-Generation RNA Sequencing of Highly Purified Human Adult and Fetal Islet Cell  
673 Subsets. *Diabetes* 2015;64:3172-3181

674 50. Peruchetti DdB, Silva-Aguiar RP, Siqueira GM, Dias WB, Caruso-Neves C: High glucose  
675 reduces megalin-mediated albumin endocytosis in renal proximal tubule cells through protein  
676 kinase B O-GlcNAcylation. *Journal of Biological Chemistry* 2018;293:11388-11400

677 51. Kim A, Knudsen JG, Madara JC, Benrick A, Hill T, Abdul-Kadir L, Kellard JA, Mellander L,  
678 Miranda C, Lin H, James T, Suba K, Spigelman AF, Wu Y, Macdonald PE, Wernstedt  
679 Asterholm I, Magnussen T, Christensen M, Visboll T, Salem V, K Knop F, Rorsman P, Lowell  
680 BB, Briant LJB: Arginine-vasopressin mediates counter-regulatory glucagon release and is  
681 diminished in type 1 diabetes. *eLife* 2021;10

682 52. Liu L, Dattaroy D, Simpson KF, Barella LF, Cui Y, Xiong Y, Jin J, König GM, Kostenis E,  
683 Roman JC, Kaestner KH, Doliba NM, Wess J:  $\alpha$ -cell Gq signaling is critical for maintaining  
684 euglycemia. *JCI Insight* 2021;

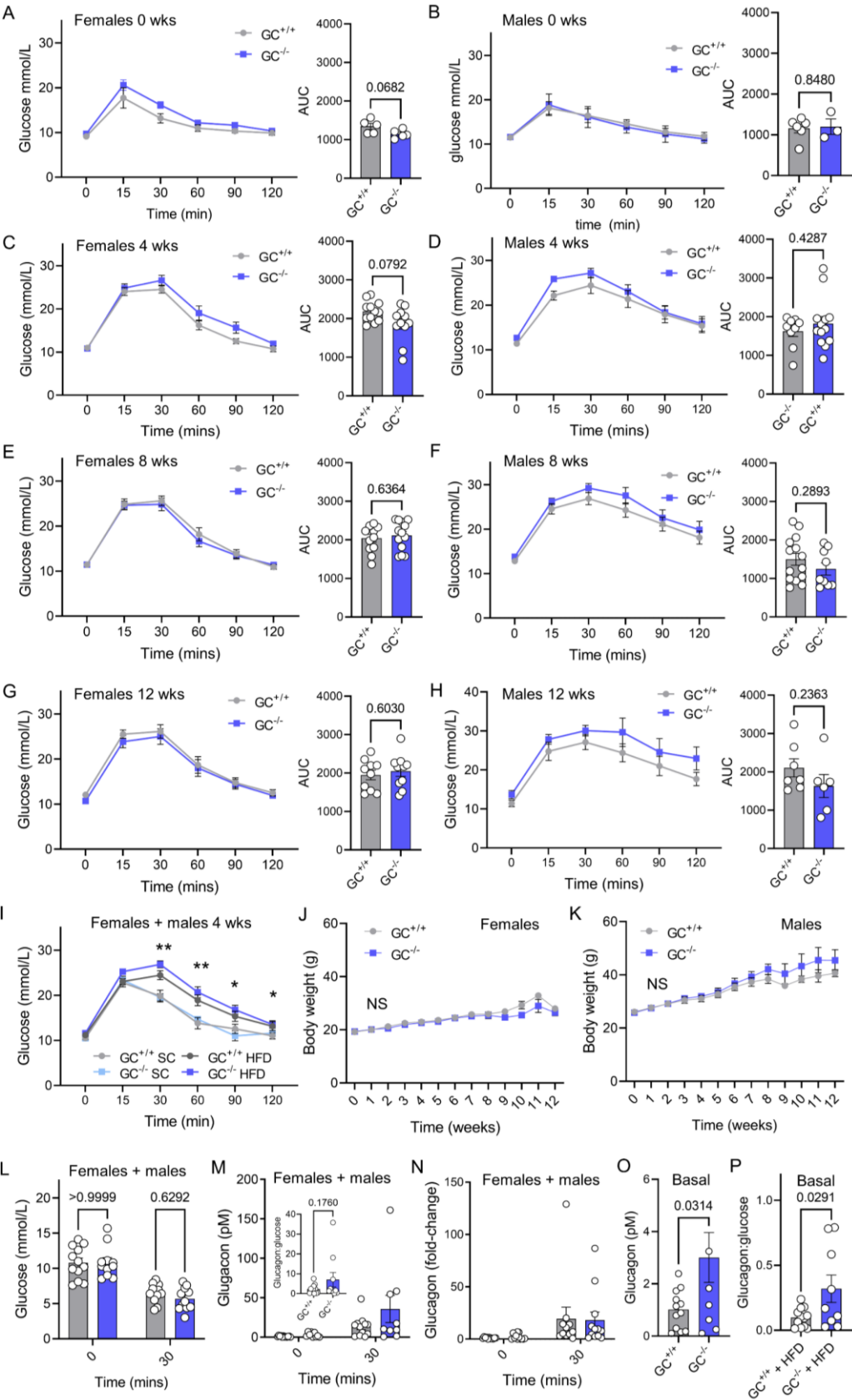
685 53. Ammala C, Drury WJ, 3rd, Knerr L, Ahlstedt I, Stillemark-Billton P, Wennberg-Huldt C,  
686 Andersson EM, Valeur E, Jansson-Lofmark R, Janzen D, Sundstrom L, Meuller J, Claesson  
687 J, Andersson P, Johansson C, Lee RG, Prakash TP, Seth PP, Monia BP, Andersson S:  
688 Targeted delivery of antisense oligonucleotides to pancreatic beta-cells. *Sci Adv*  
689 2018;4:eaat3386

690 54. Templeman NM, Flibotte S, Chik JHL, Sinha S, Lim GE, Foster LJ, Nislow C, Johnson JD:  
691 Reduced Circulating Insulin Enhances Insulin Sensitivity in Old Mice and Extends Lifespan.  
692 Cell Reports 2017;20:451-463

693 55. Page MM, Skovsø S, Cen H, Chiu AP, Dionne DA, Hutchinson DF, Lim GE, Szabat M,  
694 Flibotte S, Sinha S, Nislow C, Rodrigues B, Johnson JD: Reducing insulin via conditional  
695 partial gene ablation in adults reverses diet-induced weight gain. The FASEB Journal  
696 2018;32:1196-1206

697

698



**mice during high fat diet.** A-H) Intraperitoneal glucose tolerance is similar in female and male GC<sup>+/+</sup> and GC<sup>-/-</sup> mice during 0 weeks (A, B), 4 weeks (C, D), 8 weeks (E, F) and 12 weeks (G, H) HFD, as shown by bar graphs and AUC (0 weeks, n = 3-6 animals; 4 weeks, n = 9-13 animals; 8 weeks, n = 9-14 animals; 12 weeks, n = 6-10 animals) (two-way RM ANOVA with Sidak post-hoc test for line graphs; Mann-Whitney test or unpaired t-test for AUC). I) Pooled data from age-matched male and female mice fed SC or HFD for 4 weeks (n = 5-25 mice) (two-way RM ANOVA with Tukey's post-hoc test). J and K) Body weight gain is similar in female (J) and male (K) GC<sup>+/+</sup> and GC<sup>-/-</sup> mice during 0-12 weeks HFD (two-way ANOVA with Sidak post-hoc test). L) Glucose responses to intraperitoneal injection of insulin, used to stimulate glucagon release, are not significantly different in GC<sup>+/+</sup> and GC<sup>-/-</sup> mice at 0 mins and 30 mins (n = 11-12 animals) (two-way RM ANOVA with Sidak post-hoc test). (M and N) Basal but not insulin-stimulated plasma glucagon concentrations are significantly higher in GC<sup>-/-</sup> versus GC<sup>+/+</sup> mice, shown by raw values (M) fold-change (N) (n = 9-12 animals) (unpaired t test) (inset in M is glucagon:glucose ratio). O and P) Basal glucagon levels from (M) shown in a separate graph for clarity, alongside glucagon:glucose ratio at t = 30 mins post insulin injection (P). Glucose and glucagon readings in L-P are from the same mice, albeit with dropout of two samples in which glucagon was undetectable by ELISA. AUC, area-under-the-curve. SC, standard chow; HFD, high-fat diet.



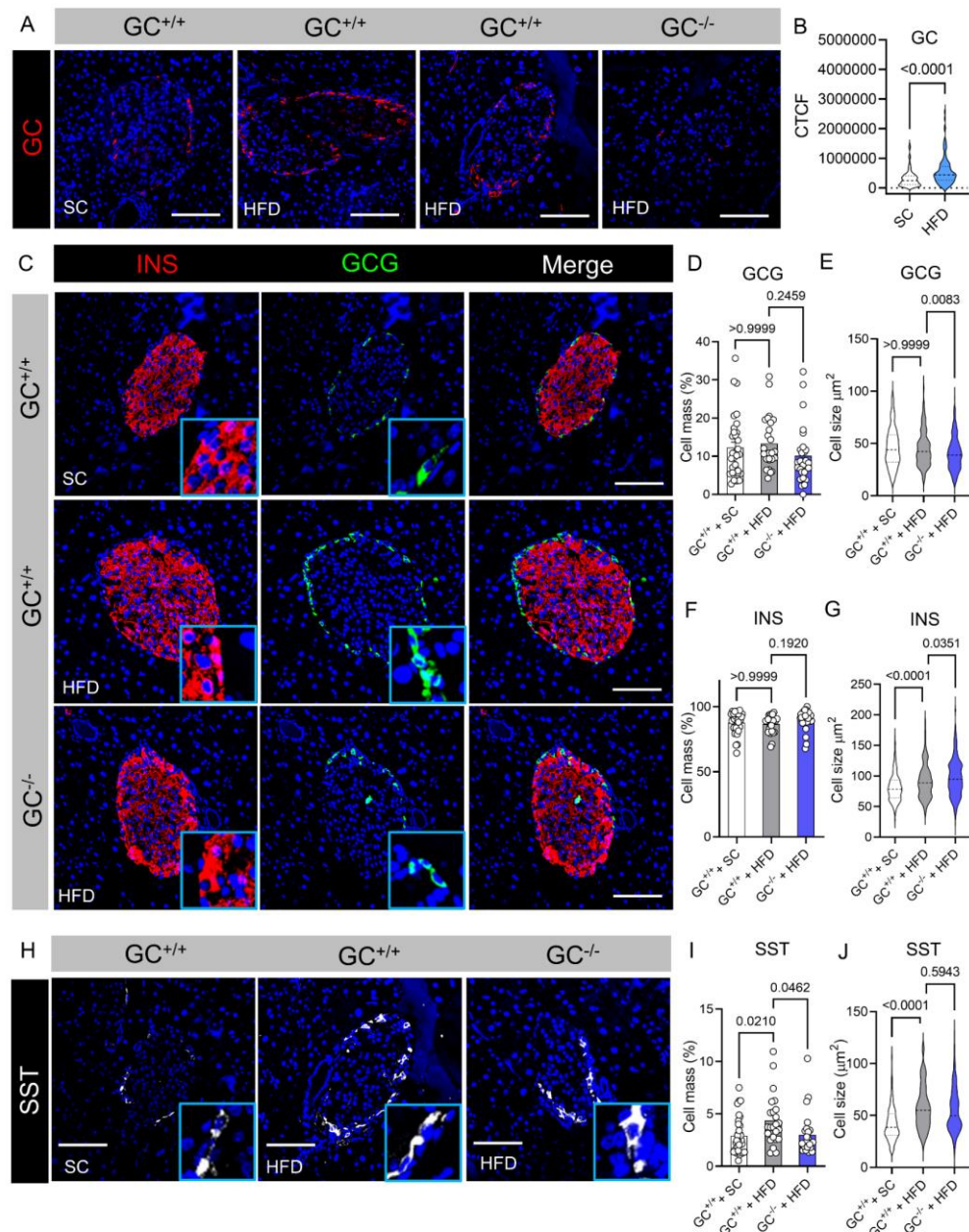


**Figure 2:  $\alpha$  cell,  $\beta$  cell and  $\delta$  cell morphometry in  $GC^{+/+}$  and  $GC^{-/-}$  mice during high fat diet.** A, B) GC expression levels are increased 2-fold following 8 weeks HFD compared to SC (A; left two image panels), quantified in (B) using corrected total cell fluorescence (CTCF). Note that immunopositivity is detected in HFD-fed  $GC^{+/+}$  and not  $GC^{-/-}$  mice, thus validating the antibody under the conditions used here (A; right two image panels). C-G) Proportion  $\alpha$  cells per islet (C, D) ( $n = 26-32$  islets from 3-4 mice), as well as  $\alpha$  cell size (C, E) ( $n = 233-301$  cells from 3-4 mice), is not affected by 8 weeks HFD in  $GC^{+/+}$  mice. Deletion of GC ( $GC^{-/-}$ ) leads to fewer and smaller  $\alpha$  cells per islet (C-E) (proportion  $\alpha$  cell per islet,  $n = 26-32$  islets

from 4 mice) ( $\alpha$  cell size,  $n = 233-301$  cells from 3-4 mice). HFD (8 weeks) does not increase proportion  $\beta$  cells per islet (C, F) ( $n = 26-32$  islets from 3-4 mice), but increases  $\beta$  cell size, an effect accentuated following deletion of GC ( $GC^{-/-}$ ) (C,G) (proportion  $\alpha$  cells per islet,  $n = 26-32$  islets from 3-4 mice) ( $\beta$  cell size,  $n = 240-320$  cells from 3-4 mice) (one-way ANOVA with Bonferroni's post-hoc test). H-J) HFD (8 weeks) increases proportion  $\delta$  cells per islets, as well as  $\delta$  cell size in  $GC^{+/+}$  but not  $GC^{-/-}$  islets ( $GC^{-/-}$ ) (proportion  $\delta$  cells per islet,  $n = 24-31$  islet from 3-4 mice) ( $\delta$  cell size,  $n = 117-294$  cells from 3-4 mice) (one-way ANOVA with Bonferroni's post-hoc test). Scale bar = 85  $\mu m$ . GC, GC-globulin, GCG, glucagon, INS, insulin, SST, somatostatin. SC, standard chow; HFD, high-fat diet.

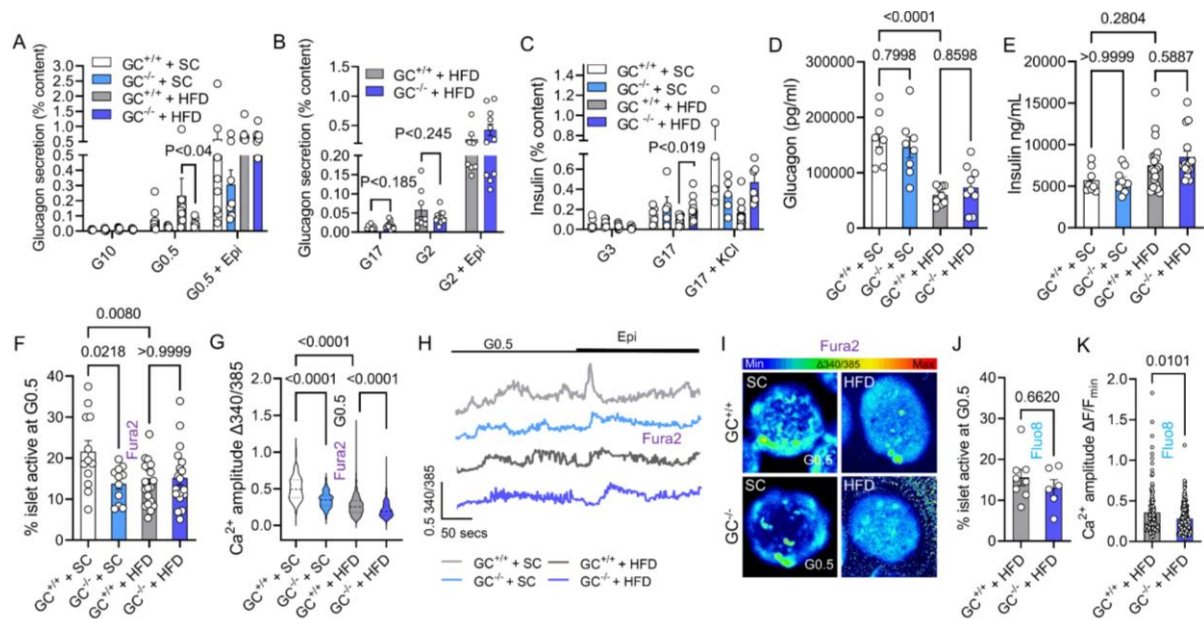


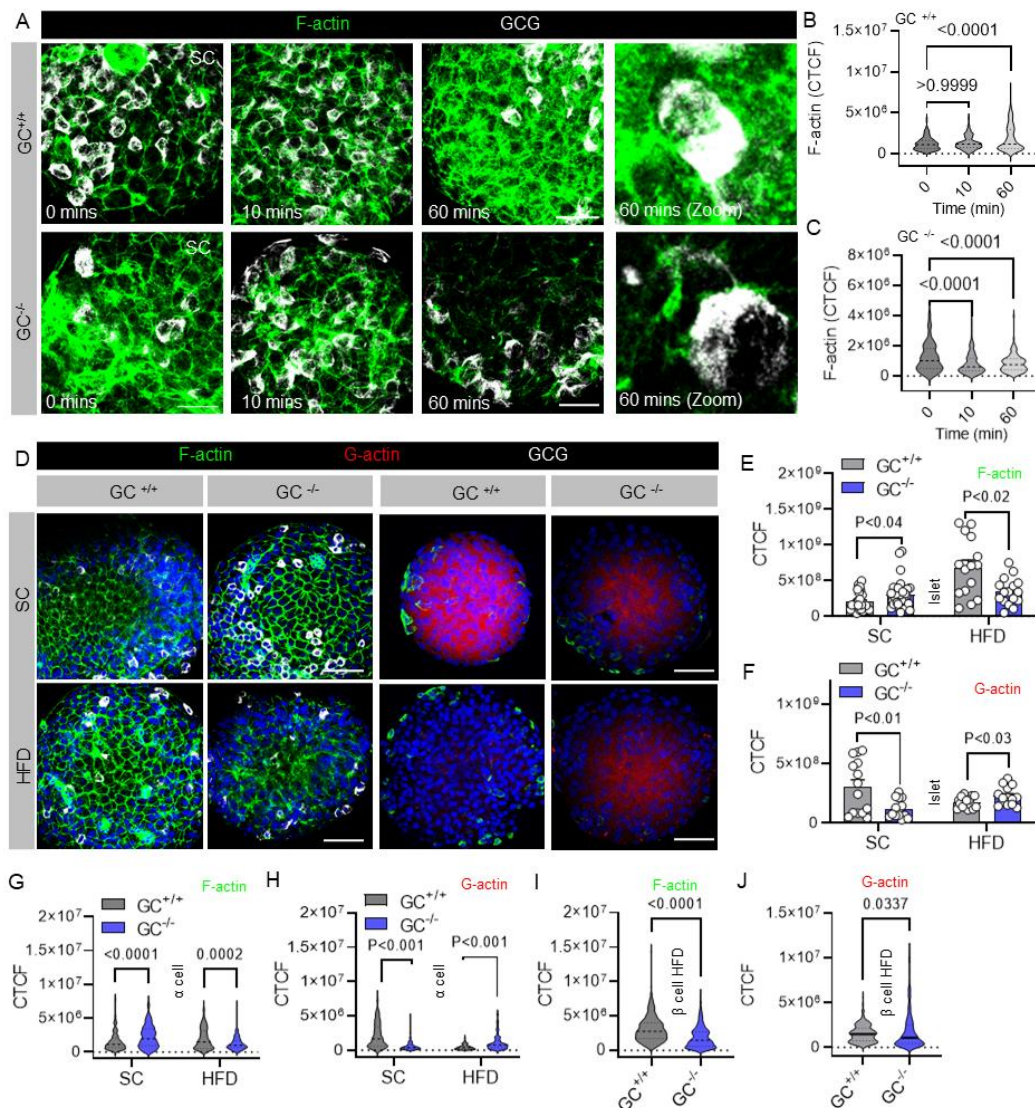
**Figure 3: Hormone secretion and ionic fluxes in islets isolated from high fat diet-fed  $GC^{+/+}$  and  $GC^{-/-}$  mice.** A) Low glucose (0.5 mM)-stimulated glucagon secretion is impaired in SC and HFD islets isolated from  $GC^{-/-}$  versus  $GC^{+/+}$  mice (SC,  $n = 4-5$  animals; HFD,  $n = 7$  animals) (Mann-Whitney test). B) As for A) but showing a tendency toward elevated basal glucagon secretion and impaired low glucose-stimulated glucagon secretion in HFD islets from  $GC^{-/-}$  versus  $GC^{+/+}$  mice ( $n = 3-4$  animals) (Student's t-test). C) Glucose-stimulated insulin secretion is significantly increased in  $GC^{-/-}$  islets isolated from HFD- but not SC-fed animals (SC,  $n = 7-8$  replicates from 3-5 animals; HFD,  $n = 7-8$  replicates from 4-5 animals) (Mann-Whitney test). D and E) Total glucagon (D) and insulin (E) concentration is similar in  $GC^{+/+}$  and  $GC^{-/-}$  islets isolated from SC and HFD-fed mice ( $n = 4-8$  animals) (two-way ANOVA with Bonferroni's post-hoc test). F) Proportion of  $\alpha$  cells active at low glucose (0.5 mM) was reduced in  $GC^{-/-}$  islets from SC-fed but not HFD-fed mice (versus  $GC^{+/+}$  littermate controls) ( $n = 11-19$  islets from 3-4 animals) (one-way ANOVA with Bonferroni's post-hoc test). G-I) Amplitude of  $Ca^{2+}$  spikes (at 0.5 mM glucose) was reduced in  $GC^{-/-}$  versus  $GC^{+/+}$  islets from mice on SC. HFD-alone reduced  $Ca^{2+}$  spike amplitude and baseline  $Ca^{2+}$  concentration, an effect accentuated by deletion of GC ( $GC^{-/-}$ ). Bar graphs (G) show summary data, traces (H) and images (I) are representative (one-way ANOVA with Bonferroni's post-hoc test) ( $n = 184-339$  cells from 3-4 animals). J and K) As for F and G, but using the non-ratiometric  $Ca^{2+}$  indicator,

762 Fluo8 (J, n = 6-8 islets from 2-3 animals; K, n = 50-79 cells from 2-3 animals) (Mann-Whitney  
763 test). GC, GC-globulin; G0.5, 0.5 mM glucose; G2, 2 mM glucose; G3, 3 mM glucose, G10,  
764 10 mM glucose; G17, 17 mM glucose. SC, standard chow; HFD, high-fat diet.

765

766





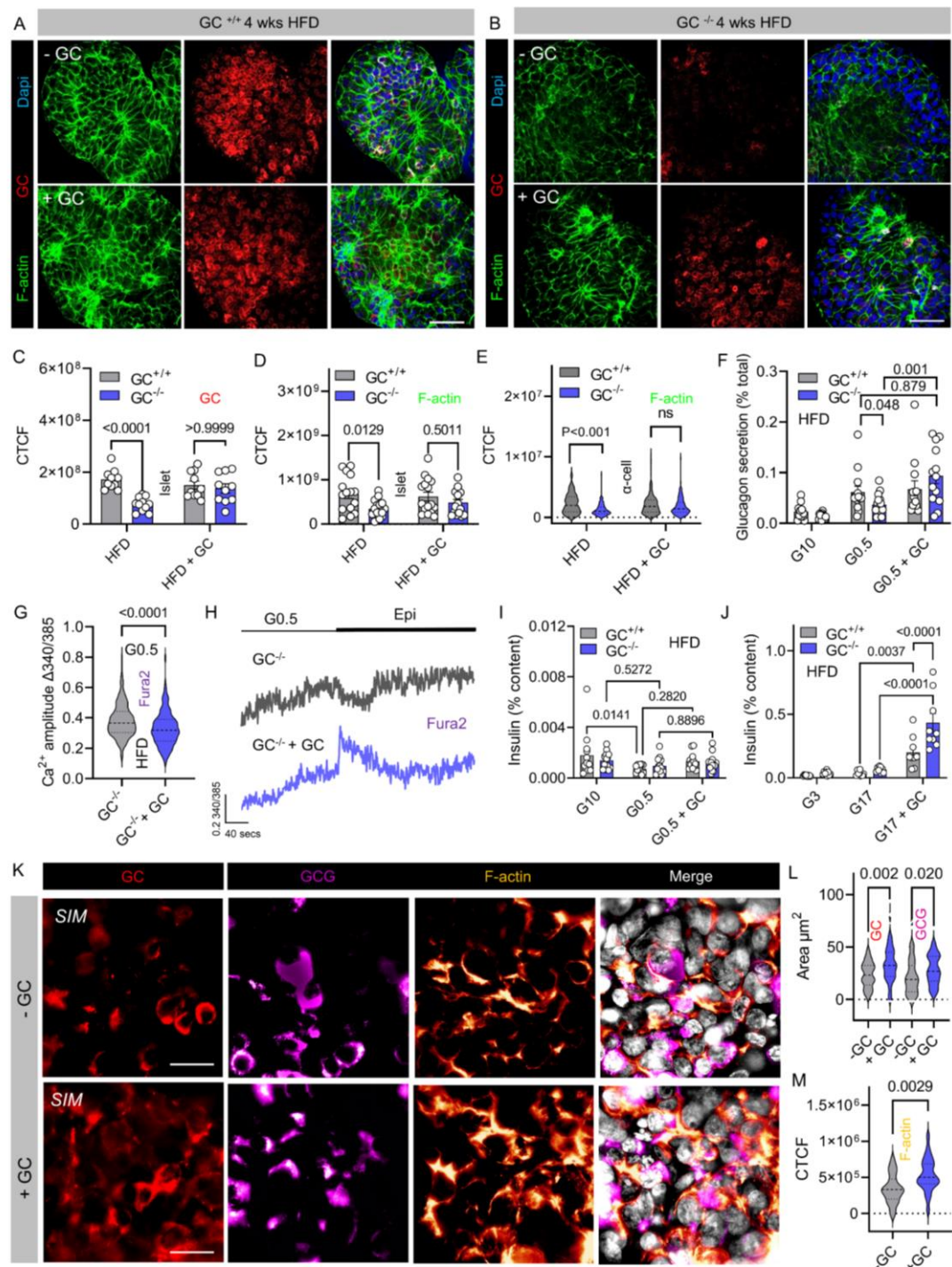
767

768 **Figure 4: F-actin and G-actin levels in islets isolated from high fat diet-fed  $GC^{+/+}$  and  $GC^{-/-}$**   
 769  **$GC^{-/-}$  mice.** (A-C) Polymeric actin (F-actin) levels increase and decrease in SC  $GC^{+/+}$  and  $GC^{-/-}$   
 770 islets, respectively, following 60 mins stimulation with low (0.5 mM) glucose concentration, as  
 771 shown by representative images (A) and summary bar graphs (B and C) ( $n = 110-145$   $\alpha$  cells  
 772 from 3 animals) (one-way ANOVA with Bonferroni's post-hoc test) (scale bar =  $34 \mu m$ ). D-F)  
 773 F-actin density is increased in  $GC^{-/-}$  islets from SC-fed mice. HFD induces a large increase in  
 774 F-actin density in  $GC^{+/+}$  islets, which can be partly reversed by deletion of GC ( $GC^{-/-}$ ).  
 775 Monomeric G-actin, which is liberated following F-actin disassembly, shows the opposite  
 776 trend. Representative images show F-actin and G-actin levels in the islet (D), analyzed in (E

777 and F) using corrected total cell fluorescence (CTCF) (Mann-Whitney test or unpaired t test)  
778 (n =15-30 islets from 3 animals) (scale bar = 53  $\mu$ m).G-J), As for D-F, but CTCF analysis of F-  
779 actin and G-actin in HFD  $\alpha$  cells (G and H) and  $\beta$  cells (I and J) (two-way ANOVA with  
780 Bonferroni's post-hoc test) (n = 159-176 cells from 3 animals). SC, standard chow; HFD, high-  
781 fat diet.

782

783



784

785 **Figure 5: Effects of exogenous GC supplementation in islets from high fat diet-fed GC<sup>+/+</sup>**  
 786 **and GC<sup>-/-</sup> mice.** A and B) Representative images showing that GC expression and F-actin  
 787 levels can only be modified in HFD GC<sup>-/-</sup> islets following incubation with GC (scale bar = 53  
 788 μm). C and D) Corrected total cell fluorescence (CTCF) analysis showing a significant  
 789 increase in GC (C) and F-actin (D) levels in GC-treated HFD GC<sup>-/-</sup>, but not GC<sup>+/+</sup>, islets (n =

10-11 islets from 3 animals) (two-way ANOVA with Bonferroni's post-hoc test). E) As D, but  
F-actin levels in individual  $\alpha$  cells (n = 10-11 islets from 3 animals) (two-way ANOVA with  
Bonferroni's post-hoc test). (F) Exogenous GC restores low glucose (G0.5)-stimulated  
glucagon secretion in HFD GC<sup>-/-</sup> islets (n = 14-16 repeats from 5-7 animals) (Mann-Whitney  
test). G and H) Exogenous GC does not affect low glucose (G0.5)-stimulated Ca<sup>2+</sup> rises in  
HFD GC<sup>-/-</sup> islets, shown by amplitude (G) and representative traces (H) (n = 174-205 cells  
from 4 animals). I) HFD GC<sup>-/-</sup> islets fail to shut off insulin secretion at low glucose, although  
GC treatment itself is unable to influence basal insulin release (n = 14 repeats from 4 animals).  
J) GC treatment amplifies glucose-stimulated insulin secretion, with a larger effect in HFD GC<sup>-/-</sup>  
compared to GC<sup>+/+</sup> islets (n = 9 repeats from 2-3 animals) (two-way ANOVA with Bonferroni's  
post-hoc test). K-M) GC levels can be supplemented in human islets (K, L), leading to an  
increase in glucagon granule area (L) and F-actin density (M). Note that the GC images are  
not from the same islets as those showing glucagon and F-actin. Scale bar = 15  $\mu$ m. GC, GC-  
globulin; GCG, glucagon; G0.5, 0.5 mM glucose; HFD, high-fat diet.



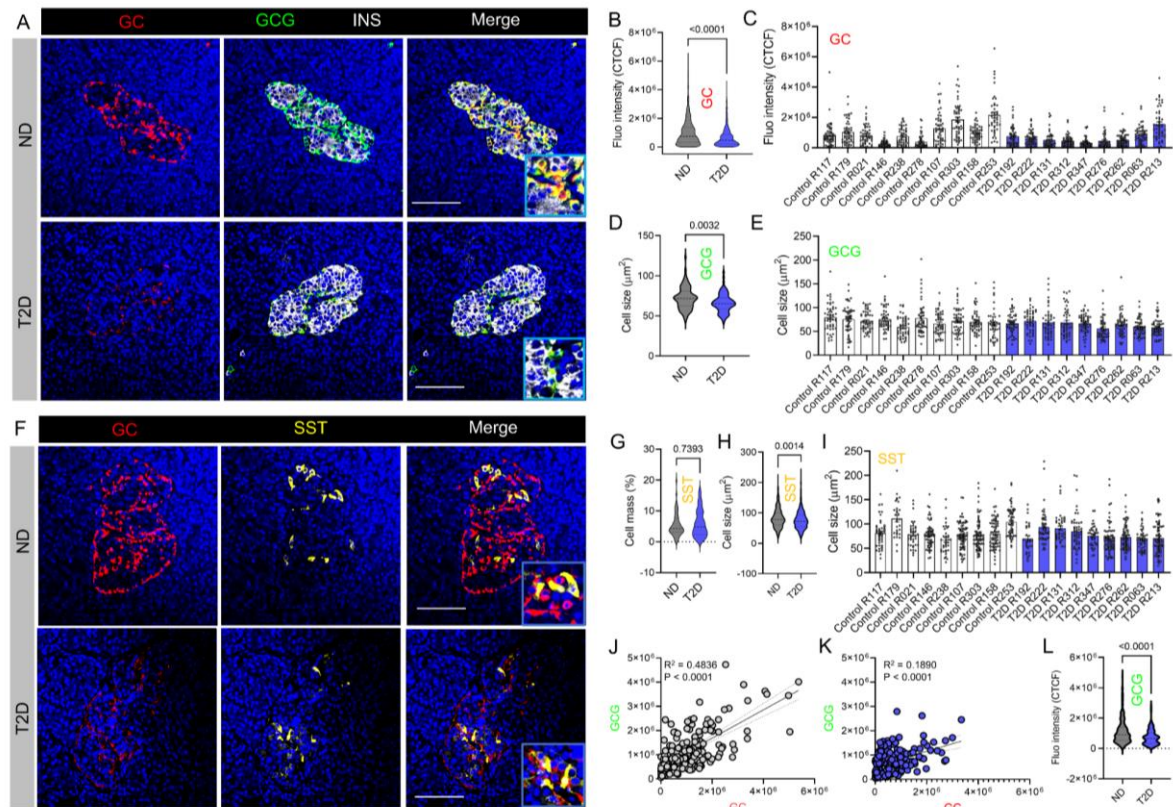


**Figure 6: GC and glucagon expression in islets from donors with and without type 2 diabetes.** A) Representative images from non-diabetic (ND) and type 2 diabetes (T2D) donors showing a large reduction in GC expression, as well as decrease in  $\alpha$  cell size. B and C) Quantification using corrected total cell fluorescence (CTCF) reveals a highly significant decrease in GC expression in T2D versus ND donors (B), which is consistent across individual donors (C) (ND, n = 89 cells from 10 donors; T2D, n = 82 cells from 9 donors) (Mann-Whitney test). D and E)  $\alpha$  cell size is significantly decreased in T2D versus ND donors (D), again consistent across donors (E) (ND, n = 495 cells from 10 donors; T2D, n = 450 cells from 9 donors) (Mann-Whitney test). F) Representative images from non-diabetic (ND) and type 2 diabetes (T2D) donors showing a large reduction in GC expression, as well as decrease in  $\delta$  cell size. (G-I)  $\delta$  cell mass (G) is similar in ND and T2D donors, whereas  $\delta$  cell size is reduced during T2D (H), consistent across individual donors (I) (ND, n = 174 islets from 9 donors; T2D, n = 210 islets from 9 donors). (J and K) GC and glucagon expression are strongly correlated in  $\alpha$  cells of ND (J), but not T2D donors (K) (linear regression). (L) Glucagon

821 expression is significantly decreased in T2D versus ND donors (ND, n = 200 cells from 10  
822 donors; T2D, n = 180 cells from 9 donors). Scale bar = 85  $\mu$ m. GC, GC-globulin, GCG,  
823 glucagon, INS, insulin, SST, somatostatin.

824

825